Supporting information

Table S1. Mobility, carrier concentration and resistivity of IGZO and In_2O_3 films

metal oxide	μ_{lin} ($cm^2 V^{-1} s^{-1}$)	Carrier concentration (cm^{-3}) Hall measurements	calculated	resistivity ($\Omega \cdot cm$)
IGZO (2:1:1)	2.2	/	7.2×10^{14}	4.6×10^{6}
In_2O_3	/	8.1×10^{15}	2.3×10^{16}	63.6

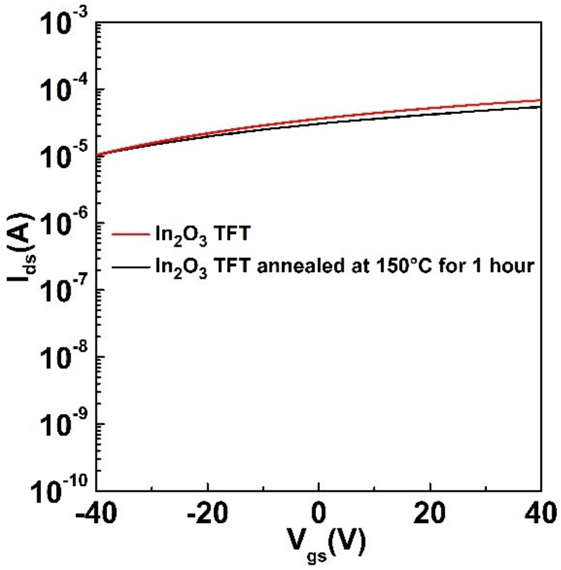

Figure S1. Transfer curve of conductive In_2O_3 TFT after annealing at 150° C for 1 hour

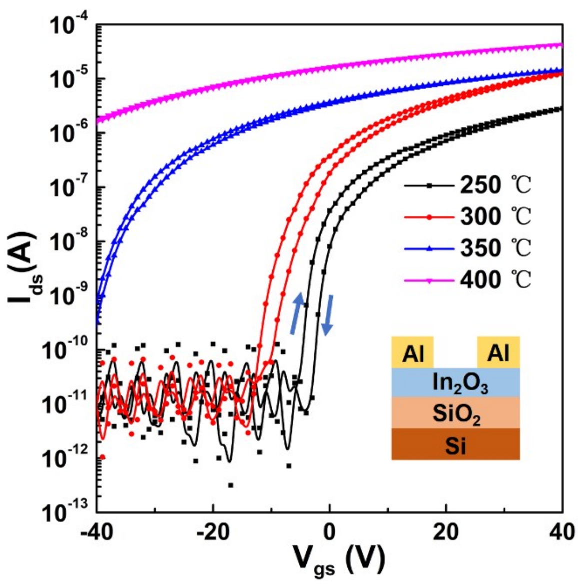

Figure S2. Transfer curves of In_2O_3 TFTs at different annealing temperatures. The insets show the device architecture employed.

Table S2. Performance of the In_2O_3 TFTs at different annealing temperatures

metal oxide	μ_{lin} (cm^2V^{-1} s^{-1})	Von (V)	$I_{on/off}$	SS ($Vdec.^{-1}$)
In_2O_3 (250°C)	3.1	-4.9	2.3×10^5	0.95
In_2O_3 (300°C)	7.6	-11.8	2.1×10^6	1.0
In_2O_3 (350°C)		Conductive		
In_2O_3 (400°C)		Conductive		

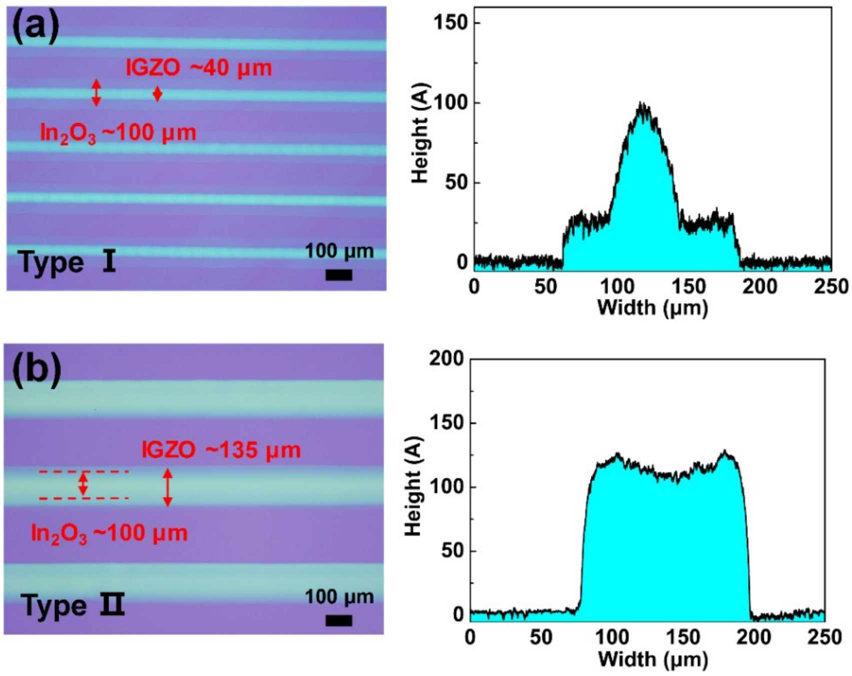

Figure S3. (a) and (b) are optical photographs and surface profiles of heterojunction channel layers of Type I and Type II devices, respectively.

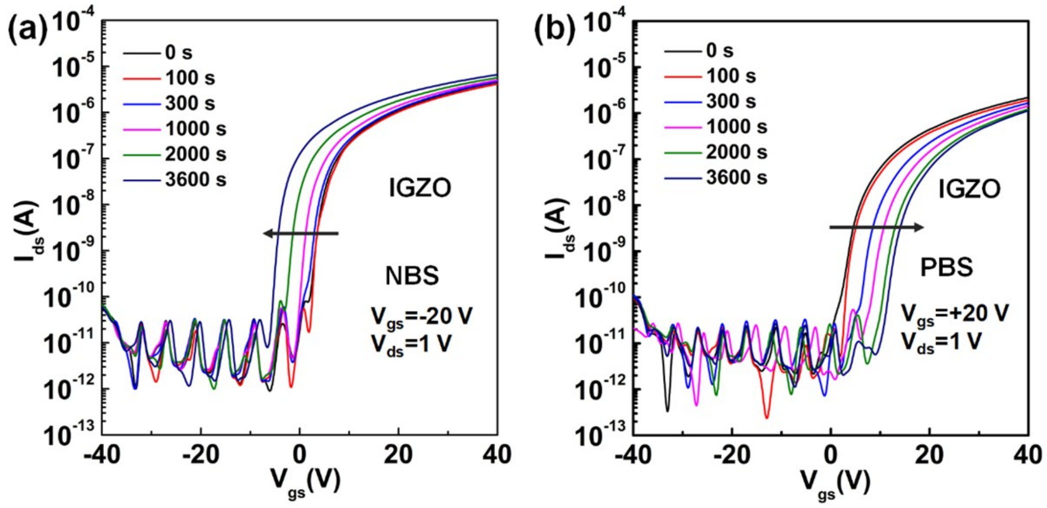

Figure S4. Transfer characteristics of IGZO TFT: (a) under NBS, (b) under PBS.

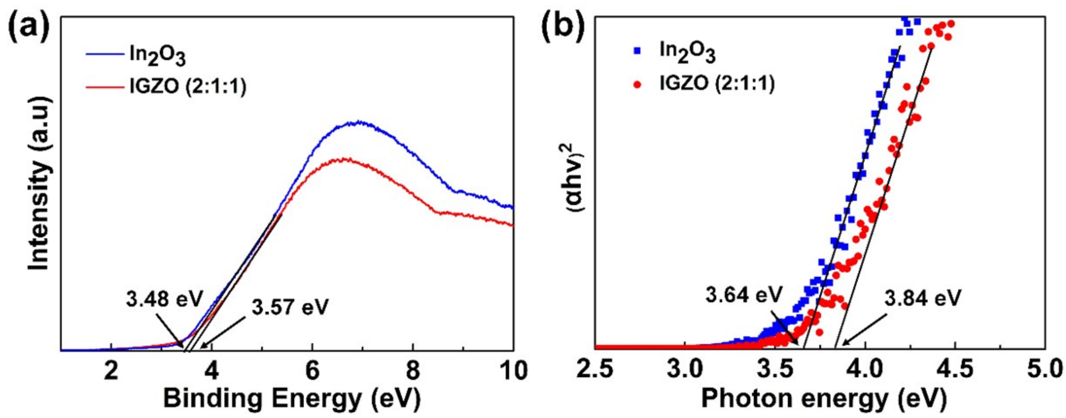

Figure S5 (a) UPS valence band spectrum of In_2O_3 and IGZO (2:1:1), black line is used to determine the upper edge of VB.(b) shows the ultraviolet absorption spectrum of the In_2O_3 and IGZO (2:1:1) films as a function of photon energy (eV), and the black line is used to determine the band gap.